Review

†Emeritus Director BIPM.
‡Present address: INMS NRC, Ottawa, Canada.
§Emeritus Principal Research Physicist BIPM.

Royal Society **Publishing**

The BIPM measurements of the Newtonian constant of gravitation, *G*

Terry Quinn[1,†], Clive Speake[2], Harold Parks[1,‡] and Richard Davis[1,§]

[1]BIPM, Pavillon de Breteuil, Sèvres Cedex 92312, France
[2]School of Physics and Astronomy, University of Birmingham, Birmingham B15 2TT, UK

This paper is a complement to the two short papers published in 2001 and 2013 in which we presented the results of the two BIPM determinations of the Newtonian constant of gravitation *G*. While this review contains no new results, it includes more detailed descriptions of certain key parameters that enter into the determination of *G*. Following a description of the overall method and the two versions of the experiment, we discuss the properties of the torsion strip, including the effects of anelasticity, then the electrostatic torque transducer, the source and test masses, dimensional metrology, angle measurement, the calculation and measurement of the moment of inertia, calculation of the torque, possible magnetic interactions and finally we discuss uncertainties and correlations in the derivation of a value for *G*.

1. Preamble

This review of the BIPM work on *G* [1,2] was undertaken in the light of the discussions that took place at the Royal Society meeting on *G* of which this issue of the *Philosophical Transactions* is the proceedings. In preparing this review, we recalculated the principal contributing parameters to our value of *G* published in 2013 [2] and in so doing, we arrived at different values for two small corrections and discovered one error. The net effect is to increase our value of *G* published in 2013 by 13 ppm and reduce its uncertainty from 27 to 25 ppm (see [2]).

(a) Introduction

The 1986 CODATA set of recommended values of the fundamental physical constants [3] included a value of

G with an estimated uncertainty of 1.3 parts in 10^4. This was a value largely based on the experiments of Luther & Towler [4] carried out in the 1970s jointly by NBS (now NIST) and the University of Virginia, published in 1982. At the time, it was well recognized that an accurate determination of G was a formidable experimental challenge, principally because the gravitational attraction between laboratory-sized masses is so small, and gravitational experiments cannot be shielded from outside gravitational perturbations. Attempts to measure G using much larger masses such as mountains, or lakes whose level can be varied, fail to produce accurate values of G, because, although the gravitational signal can be much larger than that from a laboratory experiment, the uncertainties in the gravitational coupling have always been too large. Nevertheless, there was every expectation that a value for G with an uncertainty of a part in 10^5 would likely soon be obtained.

However, confidence in the CODATA value was undermined, perhaps with hindsight incorrectly, by the publication of the result of Michaelis *et al.* [5] in 1996 which was obtained at Physikalisch-Technische Bundesanstalt (PTB; Braunschweig, Germany) using a novel method based on an electrostatic servo-controlled torsion balance floating in a mercury bath. Its estimated uncertainty was indeed a few parts in 10^5, but its value was some 0.7% higher than the CODATA value. Despite careful examination of the PTB work at the time, no source of error could be identified that would put this new value in question. In response, a number of groups around the world embarked on G experiments, including at the BIPM. Most of these are described in papers presented at the Royal Society meeting on 27 and 28 February 2014 and contained in this issue of *Philosophical Transactions A*. Despite all this work, although it is now clear that the PTB result was subjected to a serious error almost certainly in the electrostatic servo (see §3), there is still no consensus at the level of a part in 10^4 as to the value of G.

From the time of Henry Cavendish, the torsion balance using a wire suspension has been the principal device used to measure the gravitational attraction between laboratory-sized masses. It has long been considered that the principal advantage of the torsion balance over other methods is that the forces to be measured are orthogonal to those resulting from the gravitational attraction of the Earth. It was pointed out in 1895 by Boys [6] that, because the stiffness of a torsion wire increases as the fourth power of its radius, but the load capacity increases only as the square of the radius, the most advantageous configuration for high sensitivity is a very fine wire carrying a necessarily small mass. Almost all measurements of the Newtonian constant of gravitation made since then have used a torsion balance with the common design features that the fibre was a fine circular wire and the test masses were, again therefore necessarily, small. Minimizing fibre stiffness was an essential requirement before the days of optoelectronic or electronic position sensing.[1] Most of the test masses were spheres at the ends of a rod, i.e. predominantly a quadrupole mass distribution, with a total mass of the test mass assembly of a few grams. The small size of the test masses remains the case even in most modern torsion balance experiments in which the shape of the test mass is sometimes quite different. With such small test mass assemblies, the gravitational torque is very small, often of the order of $10^{-11}\,\mathrm{N\,m}$, and it is consequently very difficult to eliminate the effects of non-gravitational perturbing forces.

At the BIPM in the 1980s and 1990s, studies were carried out on the anelastic properties of Cu–1.8% Be flexure suspensions with the view to using them in high precision beam balances [7–9]. With the knowledge gained of the mechanical properties of Cu–Be flexures, the challenge presented by the PTB result for G led us to think of a torsion balance in which the test mass assembly would be suspended from a Cu–Be torsion strip [10–12]. The obvious advantage we saw at the time of the torsion strip over a torsion wire, was that the elastic torsional stiffness of a strip depends mostly on the third power of its thickness while the maximum load that can be suspended depends on the strip's cross section which, for a given thickness, can be made arbitrarily large by increasing its width (as long as the width remains much smaller

---

[1]Minimizing the elastic stiffness of a wire torsion fibre is still important in order to reduce anelasticity and ultimately the thermal noise it produces.

than the strip length). In fact, we found that for wide strips under heavy load there exists an additional gravitational restoring torque that can be much larger than the elastic component. The gravitational part of the restoring torque, being lossless, opened the possibility of designing a torsion balance having large test masses suspended from a wide torsion strip thus increasing the gravitational signal by many orders of magnitude and having a torsion balance with much higher quality factor, Q, than a fibre of the same cross section. The torsion strip design with a high-resolution sensor of angular motion therefore circumvents Boys' argument.

At the same time, we conceived the idea of using the same apparatus for three, nearly independent, methods at the same time. In every other determination of G, each experimenter has reported the result from only one method of measurement. Different experimenters have used different methods, but this is not equivalent, because the errors in one experiment are not directly constrained by the results of different methods in other experiments. In an experiment in which there are two or more independent methods underway concurrently, one has first to look for errors in each until they all agree. When this is the case, the only errors that can remain are those in the much more limited set common to all. We discuss this further in respect of our own experiment in §13. We have used two of the methods with potential for the third, and we have done the whole experiment twice with many differences in apparatus as explained below.

We begin with a description of the overall design of the BIPM G apparatus and then look in more detail at some aspects of the experiment.

(b) The overall design and operation of the BIPM G apparatus

The BIPM torsion balance (figures 1 and 2) has the following principal features which are common to the two versions labelled Mk I and Mk II with which the two results of 2001 [1] and 2013 [2] were obtained:

- a four-mass configuration to give a much reduced sensitivity to external gravitational fields, with the torque due to an external mass located far away (with respect to a characteristic length of the four-mass configuration) falling off as the fifth power of the distance compared with the third power of the distance for a dumbbell two-mass configuration. The symmetry of the suspended mass distribution also minimizes spurious torques and torsional stiffnesses owing to the coupling of simple pendulum motion, induced by ground vibration, to the torsion mode of the balance [13];
- a torsion strip to give much improved stability with practically no dependence on the material properties of the strip and the ability to suspend a much larger mass than is usual in a torsion balance while maintaining a high Q;
- a gravitational torque of about 3×10^{-8} N m, some three orders of magnitude larger than in most previous comparable measurements which improves the ratio of gravitational signal to non-gravitational and non-seismic noise and allows precise measurements to be made in a relatively short time;
- three possible modes of operation, (i) electrostatic servo control, (ii) Cavendish method, (or free deflection) method, and (iii) change in period of free oscillation, although no result was obtained with the last method as it was not possible to obtain sufficient stability of period owing to temperature variations in the laboratory (further discussed in §2);
- dimensional metrology that is quick and accurate by having the whole assembly mounted on the base of coordinate measuring machines (CMMs), with different models in the two experiments; and
- angle measurement by means of high precision autocollimators, in Mk I with a ×6 multiplying reflecting optics and in Mk II with a single direct mirror reflection (this is discussed further at the end of §6).

Figures 1 and 2 show the two versions of the BIPM G apparatus. The overall design is the same, but certain details differ resulting from the experience gained during the Mk I experiment.

Figure 1. The Mk I apparatus: (A) one of the four source masses ($\approx$11 kg); (B) one of the four test masses ($\approx$1.2 kg); (C) the torsion disc about 30 cm in diameter; (D) the central tower holding mirrors, down the centre of which is suspended the torsion strip, just visible; (F) one of the three mirror supports part of the $\times$6 multiplying optics; (G) the autocollimator; and (H) the carousel.
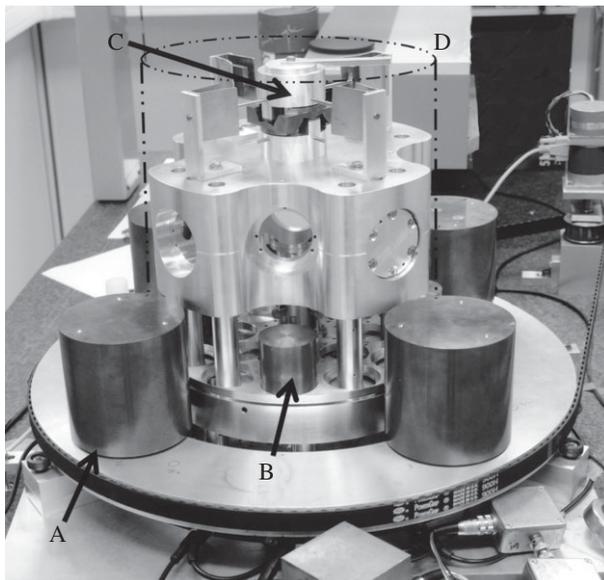

Figure 2. The Mk II apparatus, similar in principle to the Mk I: (A) one of the four source masses, used in the Mk I except that their height had been reduced by 3 mm; (B) one of the test masses, newly manufactured but similar in size to the Mk I test masses; (C) the gimbal from which is suspended the torsion strip; and (D) the autocollimator, a different model from the Mk I.

The torsion balance suspension is a Cu–1.8% Be ribbon from which hangs a torsion disc of aluminium alloy in which holes with a range of diameters were machined to reduce its mass. The holes are symmetrically placed in order to eliminate their coupling to the source masses. The detailed design differed in the two experiments. Symmetrically placed around the periphery of the disc are the four test masses of Cu–0.7% Te free-machining alloy each with a mass of about 1.2 kg. The total mass of the suspended torsion balance in both experiments was about 6.6 kg with a period of about 120 s and a typical Q, in the vacuum achieved, of between 1 and 3×10^5. As we shall see, 97% of the restoring torque of the loaded torsion strip is gravitational, which is lossless, and only 3% of the total stiffness is due to the elasticity of the strip. This essentially eliminates the problem of frequency-dependent stiffness owing to anelasticity and provides a suspension with extraordinary stability and low drift. In the Mk I version, the strip was suspended directly from the top plate of the apparatus. In the Mk II version, it was suspended via a cross-knife gimbal to protect it from the effects of ground tilt and to allow the simple pendulum mode of oscillation to be damped (this is further discussed at the end of this section). An electrostatic torque actuator was designed such that the capacitance between rod electrodes and the test masses versus angle was linear with $dC/d\theta$ a maximum. Given that this implies that $d^2C/d\theta^2$ is nominally zero, potentials of the order of hundreds of volts could be applied between the electrodes and the balance without instabilities. The same design was used in both experiments.

In the Mk II version, a central pillar with four mirrors, for gravitational and inertial symmetry, is attached to the torsion balance to allow an external autocollimator to observe the position of the torsion disc by direct reflection from one of the mirrors.

Just outside the aluminium alloy vacuum chamber, which houses all of this, is a circular carousel upon which are placed four source masses, of the same material as the test masses, each having a mass of about 11 kg. The carousel is constructed from aluminium alloy, rests on three ball races and is held in place by three others on its periphery. It can be turned via a belt driven by a stepper motor to place the set of four masses in different positions with respect to the test masses on the torsion balance. When aligned radially with the test masses, the source masses produce no torque on the balance. When turned in either direction by about 18.9°, the gravitational torque is at its maximum, about 1.7×10^{-8} N m. The source masses in the Mk II experiment were the same as those used in the Mk I except that 3 mm had been removed from one end in order to re-cut the V-grooves required for the kinematic mounting of the masses on the carousel (see §4). Each source mass could be turned to sit in any one of three positions 120° apart about a vertical axis. By making measurements at the three different orientations of the source masses, calculations of the effects of the measured density inhomogeneities were checked. The test masses, newly made for the Mk II apparatus, rested on the torsion disc in 5 mm deep circular holes cut into the disc and machined to be a close fit to the masses. They were firmly held by a spot of cyanolyte ('super') glue. The orientations of the test masses were not varied as the effects of the measured density inhomogeneities in these smaller masses were considered negligible.

In the servo method, the gravitational torque is balanced by an electrostatic torque applied to the test masses, so that the torsion balance does not rotate. The torque can then be determined in terms of the changes of the cross-capacitances with angle and the voltages applied to the torque actuator

$$\tau_{\mathrm{s}} = \frac{1}{2} \sum_{i,j} \frac{dC_{ij}}{d\theta} (V_i - V_j)^2. \tag{1.1}$$

In our apparatus, there are three cross-capacitances, namely between the two electrodes and between each electrode and the rest of the apparatus. The quantities $dC_{ij}/d\theta$ are found by measuring each capacitance as a function of angle. Then, we find $G = \tau_{\mathrm{s}}/\Gamma$, where Γ is the gravitational coupling between the torsion balance and source masses. By holding the balance at a fixed angular position during the torque measurements, anelastic effects in the suspension are eliminated, although in the case of the Cavendish method anelastic effects are not significant in our apparatus, as discussed in §2. Figure 3 illustrates the sequence of operations during the servo and Cavendish runs to obtain one data point.
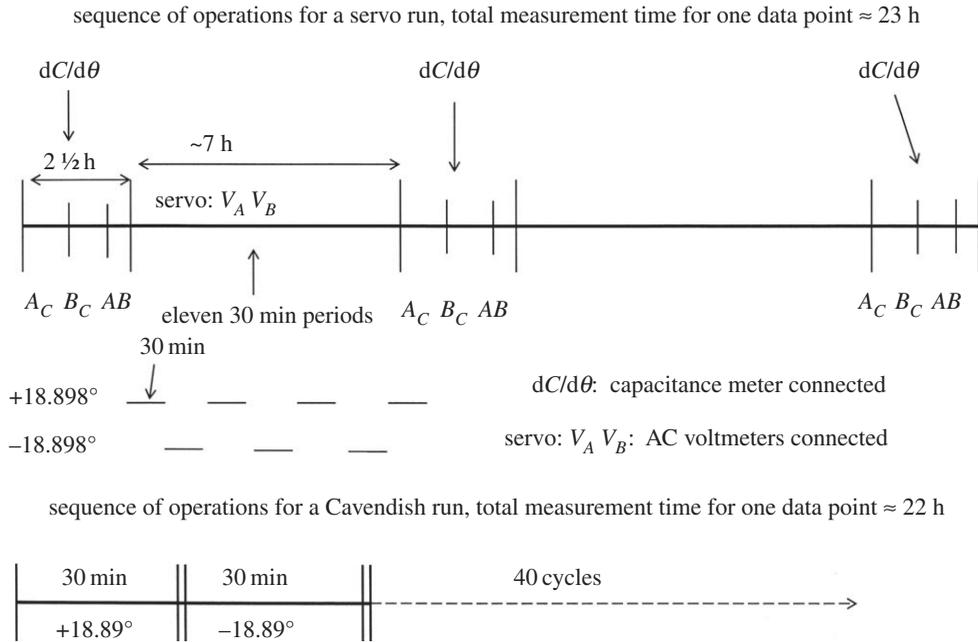
Figure 3. Timeline of operations during servo and Cavendish data collection.

In the Cavendish method, the torsion balance is allowed to rotate in response to the gravitational torque of the source masses. The peak-to-peak amplitude, $\Delta\theta_c$, of the rotation is very small, some 30 as (arc seconds) or some 150 μrad. At equilibrium, the gravitational torque is balanced by the stiffness of the suspension. The angular deflection measured by an autocollimator is related to the torque by Hooke's law, $\tau_c = k\Delta\theta_c$, where k is the stiffness of the suspension. In addition, $\tau_c = G\Gamma$, where Γ is nominally the same function of the mass distribution as in the servo method. We obtain k from measurements of the period of free oscillation T_0, with the source masses in their maximum torque position, and the moment of inertia I of the suspended system using the relation $k = I(2\pi/T_0)^2$. Common to both methods is the calculation of Γ, the gravitational interaction between the source masses and the whole torsion balance assembly, principally the test masses and discussed in §9.

A simple comparison between the two methods can be obtained from the following approximate expressions for the torques: for the servo method the torque, τ_s, is given by equation (1.1) so that $G \equiv \tau_s/\Gamma$; however, for the Cavendish method

$$\tau_c \equiv I\left(\frac{2\pi}{T_0}\right)^2 \Delta\theta_c, \tag{1.2}$$

so that $G \equiv I(2\pi/T_0)^2\Delta\theta_c/\Gamma$.

Two useful deductions can be made from a comparison of equations (1.1) and (1.2). First, angle θ appears in the denominator of the servo method and in the numerator of the Cavendish method, so that a common calibration error in θ can be eliminated in the average of the two. Second, because the mass of the test masses appears in both I the moment of inertia of the torsion balance and in the gravitational coupling Γ between the source masses and the torsion balance, it is eliminated in the Cavendish method. As we shall see, the values of Γ are slightly different for the servo and Cavendish methods.

2. The torsion strip

The key novelty in the BIPM torsion balance is the thin heavily loaded torsion strip made from a dispersion-hardened Cu–1.8% Be alloy. The shape is shown in figure 4. It is of thickness $t = 30\,\mu\text{m}$, width $b = 2.5\,\text{mm}$ and length $L = 160\,\text{mm}$. At each end, the strip widens to 20 mm over a length of 30 mm in order to provide the large surface which is clamped tightly to the gimbal support (Mk II) at the top and to the torsion disc at the bottom, as shown in figure 4. In this way, clamping occurs where there is no strain thus avoiding stick–slip losses that otherwise would lower the Q [8]. The strips were made by electrochemical machining from a rolled sheet of the un-annealed alloy in its solid solution state. Each strip could be detached from the sheet by breaking a few fine attachments located around the wide portions at the ends. It was then annealed at 330°C, while pressed between glass plates, for about 2 h. This has the effect of precipitating the beryllium into a fine dispersion throughout the material which acts as the blocking mechanism for the movement of dislocations and hence transforms it into a hard, spring material. On loading with the 6.6 kg torsion balance, the strip is operating at about 70% of its yield stress and extends by about 1 mm. Under these conditions, the suspended torsion balance is almost completely unaffected by small tilts of the top suspension. This is because, in the presence of a tilt about an axis orthogonal to the wide dimension of the strip, the small raising and lowering of opposite edges of the strip at the top are completely absorbed by the much larger extension owing to the loading stress. Tilts about an orthogonal axis to this would not be expected to produce a torque due the low stiffness of the strip to bending about this axis. We, nevertheless, included the gimbal in the Mk II version as an additional modification to the Mk I version. We did this for the following reasons. First, we had demonstrated a coupling of suspension tilt to balance rotation in an earlier version of the experiment [10] at the level of 0.4% of the rotational stiffness. This would require a tilt of amplitude of 0.4 μrad, correlated with the source mass motion, in order to produce a rotation of 10 ppm of that due to the gravitational torque. There was, however, no evidence for this actually quite large tilt being present in the Mk I experiment. Second, we believed that the random torque noise in the Mk I experiment was in part due to the large Q of the simple pendulum mode of the torsion balance. We therefore decided to use a damper in the Mk II experiment and our favoured design of damper was based on a gimbal suspension.

The restoring torque [11], k, of the loaded torsion strip with $b \gg 3t$ has an elastic component

$$k_\text{e} = \frac{bt^3 F}{3L}, \tag{2.1a}$$

and a gravitational component

$$k_\text{g} = \frac{M_\text{p} g b^2}{12L}, \tag{2.1b}$$

with

$$k = \frac{bt^3 F}{3L} + \frac{M_\text{p} g b^2}{12L}, \tag{2.1c}$$

where F is the shear modulus of Cu–1.8% Be; M_p is the total mass supported by the strip; and g is the local value of the Earth's acceleration due to gravity.

The elastic stiffness of our torsion strip has an approximate value of $7.5 \times 10^{-6}\,\text{N m rad}^{-1}$ and the gravitational component a value of approximately $2.18 \times 10^{-4}\,\text{N m rad}^{-1}$ for a load of 6.6 kg, assuming a value for the shear modulus of 53 MPa. This compares with the measured value of the restoring torque of $2.06 \times 10^{-4}\,\text{N m rad}^{-1}$ assuming a resonant oscillation period of 121 s and the measured/calculated moment of inertia of $0.076233\,\text{kg m}^2$.

Following extensive studies of the anelastic properties of this Cu–Be alloy for the purposes of flexure suspensions for balances [12], we can write the frequency dependence of the shear modulus

$$F(\omega) = \left(F_0 + \frac{\delta F}{\ln(\tau_\infty/\tau_0)} \left[\frac{1}{2} \ln \left(\frac{1 + \omega^2 \tau_\infty^2}{1 + \omega^2 \tau_0^2} \right) + i \left(\tan^{-1}(\omega \tau_\infty) - \tan^{-1}(\omega \tau_0) \right) \right] \right), \tag{2.2}$$
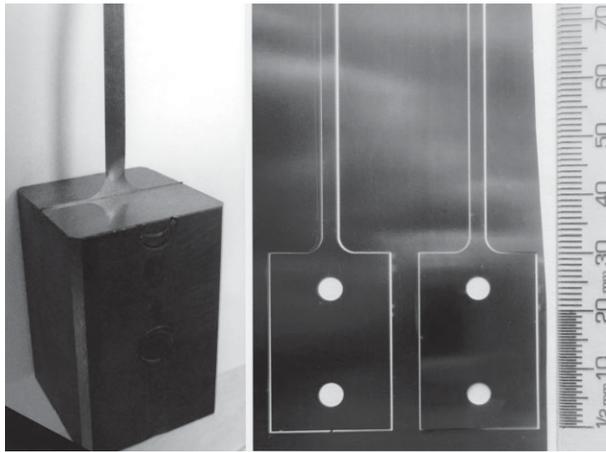
Figure 4. The torsion strip and its mounting. On the RHS, two strips can be seen not yet taken from the sheet of 30 μm thick Cu–1.8% Be and on the LHS a strip showing how it is held at its wide ends to avoid strain when it is clamped (see text for further explanation).

where τ_0 and τ_∞ are, respectively, the shortest and longest time constants characterizing the loss mechanisms in the flexure and ω is the angular frequency of stress variations in the flexure produced by the torsional oscillations of the balance. The quantity δF is the relaxation strength of an individual relaxation mechanism in the spectrum. The equation of motion of the torsion balance can be written, in the absence of viscous damping, as

$$I\ddot{\theta} + 2\gamma I\dot{\theta} + k_r\theta = N, \qquad (2.3a)$$

where, again, I is the moment of inertia of the torsion balance, γ is a frequency-dependent damping coefficient, k_r is the real part of the restoring torque and N is an applied torque. From equations (2.1) and (2.2) and noting that $\delta F \ll F_0$, we can write

$$k_r = \frac{Mgb^2}{12L} + \frac{bt^3}{3L}\left[F_0 + \frac{\delta F}{2\ln(\tau_\infty/\tau_0)}\ln\left(\frac{1+\omega^2\tau_\infty^2}{1+\omega^2\tau_0^2}\right)\right] \qquad (2.3b)$$

and the damping constant becomes

$$\gamma = k_e\frac{\delta F/F}{2I\omega\ln(\tau_\infty/\tau_0)}(\tan^{-1}\omega\tau_\infty - \tan^{-1}\omega\tau_0). \qquad (2.3c)$$

In free oscillation, with $N = 0$, equation (2.3a) can be solved in the usual way to calculate the natural angular frequency of oscillation,

$$\omega_R = (\omega_0^2 - \gamma^2)^{1/2} \qquad (2.4)$$

with

$$\omega_0^2 = \frac{k_r(\omega_0)}{I}. \qquad (2.5)$$

Given that the gravitational restoring torque is significantly larger than the elastic term and that the lossy component of the elastic term is suppressed by the modulus defect, we can assume that $\omega_R = \omega_0$. We use equation (2.3b) to estimate the stiffness at the resonant frequency, $k_r(\omega_0)$, and the stiffness, $k_r(\omega_m)$, at the angular frequency, ω_m, that the gravitational torques are applied to the balance during the measurements. The difference between these two stiffnesses can be written

$$k_r(\omega_m) - k_r(\omega_0) = \frac{bt^3}{3L}\frac{\delta F}{2\ln(\tau_\infty/\tau_0)}\ln\left(\frac{1+\omega_m^2\tau_\infty^2}{1+\omega_0^2\tau_\infty^2}\right), \qquad (2.6a)$$

where we have assumed that $\omega_0\tau_0, \omega_m\tau_0 \ll 1$ which is consistent with observations [8]. If we further suppose that $\omega_0\tau_\infty, \omega_m\tau_\infty \gg 1$, which implies that we are still in the regime where the full spectrum of damping processes has not relaxed during the data taking runs, we find

$$k_r(\omega_m) - k_r(\omega_0) = k_e \frac{\delta F/F}{\ln(\tau_\infty/\tau_0)} \ln\left(\frac{T_0}{T_m}\right),\tag{2.6b}$$

with $T_0 = 2\pi/\omega_0 = 121\,\mathrm{s}$ and $T_m = 2\pi/\omega_m = 1800\,\mathrm{s}$. In the same frequency regime, we find that the damping constant given in equation (2.3c) can be written

$$\gamma = \frac{1}{2I\omega} k_e \Delta,\tag{2.6c}$$

where $\Delta = (\delta F/F)(\pi/2\ln(\tau_\infty/\tau_0))$. The quantity Δ for Cu–1.8% Be at the appropriate stress has been measured to be $1.0(2) \times 10^{-4}$ [8,14]. The fractional bias in the value of G owing to anelasticity can be written

$$\frac{\delta G_{an}}{G} = \frac{k_r(\omega_m) - k_r(\omega_0)}{k_e + k_g} = \frac{2}{\pi} \frac{k_e \Delta \ln(T_0/T_m)}{k_e + k_g}.\tag{2.7}$$

This leads to a correction to G when calculated using the stiffness at resonance of $-5.9\,\mathrm{ppm}$. The importance of equation (2.6a) was pointed out by Kuroda [15] and its implications in time of swing experiments have become known as the 'Kuroda effect'. Our 2013 value for G included, as did the 2001 value, a correction for anelasticity of $-13\,\mathrm{ppm}$ with an uncertainty of $4\,\mathrm{ppm}$. We now believe that this correction was an overestimation based on our anelasticity data and should be only $-6\,\mathrm{ppm}$ with a conservative uncertainty of $6\,\mathrm{ppm}$.

Because the second term in equation (2.1) does not contain the modulus of elasticity, it should be independent of material properties and thus lossless. We confirmed this in experiments [8] in which we showed that under heavy load, in which the second gravitational term represented nearly 99% of the restoring torque, it was possible to make a torsion balance supporting a load of 10 kg having a period of 18 s with a Q of 1.24×10^6. This was only slightly below the expected value, the difference being attributable to losses at the ends, which were not optimally designed, and residual viscous damping in the vacuum that we could achieve. We also note that the time-dependent relaxation after deflection of a torsion balance, the anelastic after-effect, is also proportional to Δ [7,12].

The origin of the second, gravitational term is the fact that as the torsion strip turns the lower end rises. The potential energy thus gained supplies the restoring torque. For an angular deflection θ, the potential energy of the suspended mass, M_p, increases by an amount given by

$$\frac{1}{2}k_g\theta^2 = \frac{M_p g b^2}{24L}\theta^2.\tag{2.8a}$$

This can be due only to the mass being raised to a height Δh above its rest position

$$M_p g \Delta h = \frac{M_p g b^2 \theta^2}{24L},\tag{2.8b}$$

so that

$$\Delta h = \frac{b^2}{24L}\theta^2.\tag{2.8c}$$

For small angular deflections, Δh can be very small. In the present G experiment, in which the deflection of the torsion balance during the Cavendish mode is about $150\,\mu\mathrm{rad}$, we find Δh is only 10 fm (which is roughly the diameter of the nucleus of a copper atom).

It is interesting to note that Heyl & Chrzanowski [16] attempted to exploit the properties of a bifilar suspension that provides an apparently similar gravitational restoring torque. In fact, there is a crucial difference. In a wide torsion strip, the strain is distributed uniformly along the length of the strip, whereas in a bifilar suspension all of the strain occurs at the points of attachment of the wires where it is impossible to avoid frictional losses.

For a wire suspension, the equivalent expression for restoring torque is

$$k_w = \frac{\pi r^4}{2L}\left(F + \frac{M_p g}{\pi r^2}\right), \tag{2.9}$$

where $M_p g/\pi r^2$ is the stress, σ, in the wire. Because σ is always much smaller than F, the restoring torque is always dominated by the elastic component, so that a torsion balance suspended on a wire can never have the high Q of one suspended on a torsion strip.

The ratio of the restoring torque of a strip, k, and a wire k_w having the same length, same shear modulus and ultimate stress, the same test mass load and the same cross section, i.e. $\pi r^2 = bt$, is thus given by

$$\frac{k}{k_w} = \frac{k_e}{k_w} + \frac{k_g}{k_w} \approx \frac{2\pi}{3}\left(\frac{t}{b}\right) + \frac{\pi}{6}\frac{\sigma}{F}\left(\frac{b}{t}\right). \tag{2.10}$$

For the torsion strip used in the G work, in which $b/t = 83$, the ratio k/k_w is, from the second term in equation (2.10), about 0.7. Thus, the period of oscillation of the two balances with equal loads and therefore gravitational signal in a G experiment, will be about the same. However, the anelastic after-effect and the damping would be larger, from the first term in equation (2.10), by a factor of about 40 in the wire torsion balance. In addition, there would most likely be additional damping owing to stick–slip associated with the clamping of the ends of such a stiff wire. The amplitude spectral density of thermal noise torques, n_T, acting on a torsion balance due to anelastic losses in the suspension gives rise to $1/f$ noise [12],

$$n_T = \left(4k_B T \frac{k_e}{\omega_m}\Delta\right)^{1/2} \mathrm{N\,m\,Hz}^{-1/2}, \tag{2.11}$$

where ω_m is the cadence of the experiment and, for the torsion wire, we can write k_w for k_e. The signal-to-noise ratio will be more favourable by the square root of the ratios of the elastic stiffness or, for our example, by a factor of about 6. We can see that the torsion strip provides a significantly better performance than the torsion wire in the case where the experimental uncertainty is dominated by non-gravitational forces, i.e. where the signal to noise is proportional to the test mass value. The disadvantage of the torsion strip is that its angular displacement compared with a wire-suspended balance is reduced owing to its increased effective stiffness, and the sensitivity can be limited by the noise level in the detector of angular displacement.

We can extend Boys' argument to encompass the torsion strip design in the following way. Imagine a wire and a strip suspension with their respective detectors of angular displacement and suppose that the suspensions have the same elastic stiffnesses ($k_e = k_w$), then they will have equal intrinsic anelasticity, defined say by the magnitude of the anelastic after-effect. The ratio of the gravitational signals in a G experiment, determined by the values of their test masses, will be proportional to the square root of the aspect ratio of the torsion strip. This follows from the first term in equation (2.11). In our case, this is again about a factor of 6 in favour of the torsion strip. In order for the torsion strip and its detector to fully exploit this gain in signal, the detector must have a noise level that is better by a factor of k_g/k_w (the second term in equation (2.11)) or about 40 in our case. A further point is that the higher stiffness of the torsion strip broadens its useful frequency range and gives the possibility of working at a higher ω_m with reduced $1/f$ noise.

We noted in §1 that we were unable to use the time-of-swing method to give a precise value of G owing to the lack of temperature stability in our laboratory. We can estimate the temperature coefficient of the restoring torque given the temperature coefficients of the shear modulus and of the strip dimensions. If we define α as the coefficient of thermal expansion of the strip and the fractional change in the shear modulus as

$$\eta = \frac{1}{F}\frac{dF}{dT}, \tag{2.12}$$

then the rate of change of the restoring torque of the torsion strip with temperature becomes

$$\frac{1}{k}\frac{dk_e}{dT} \approx (3\alpha - \eta)\frac{k_e}{k_g} + \alpha. \tag{2.13a}$$

With $\eta = -4 \times 10^{-4}$ [14] and $\alpha = 17 \times 10^{-6}$, we find that $1/k.dk_e/dT \sim -5 \times 10^{-6}\,\mathrm{K}^{-1}$, with the temperature coefficient of the gravitational component being mostly compensated by that of the elastic component. We can, for completeness, calculate a similar expression for a wire suspension,

$$\frac{1}{k_w}\frac{dk_w}{dT} = (3\alpha - \eta),\tag{2.13b}$$

which is dominated by the thermal dependence of the elastic modulus. Using equations (2.13a) and (2.13b), the ratio of the sensitivity of the strip to the wire to temperature variations is $\sim (k_e/k_g) - (\alpha/\eta)$. Noting that the period change is proportional to square root of the ratio of the moment of inertia to the torsional stiffness, we can calculate the fractional change in the period, P, as

$$\frac{1}{P}\frac{dP}{P} = \alpha_P - \frac{1}{2k}\frac{dk_e}{dT},\tag{2.14}$$

where α_P is the thermal expansion coefficient of the torsion disc.

We can estimate the change in the stiffness of the torsion pendulum due to the gravitational torque of the source masses when they are at their closest to the test masses by differentiating equation (5.1) below,

$$k_G \approx 140\,GMm\,\frac{r^4}{R^5}.\tag{2.15}$$

Using equations (2.13a) and (2.14), we can estimate that the stability of the temperature required to achieve 10 ppm in G is about 0.5 mK. This level of control is possible in a state-of-the-art laboratory with a good experimental thermal design; however, we were unable to achieve this over periods long enough to enable us to obtain data with high enough quality to derive a value for G.

Some data were taken using the time of swing method. The measured change in period was about 37 ms with a standard deviation of 9 μs, equivalent to a relative uncertainty in G of about 250 ppm. The variation in laboratory temperature while these data were being taken was $\pm 0.15^\circ$C, from which one can deduce that to reach an uncertainty in G of 10 ppm we would need a stability of temperature of about 6 mK, which is in reasonable agreement with the calculations above given that the thermometers were just outside the vacuum can. The absolute value of the period of 120 s during these data varied with a standard deviation of about 250 μs or 2 ppm which was more than adequate for the timing in the other configurations.

With a stable enough temperature, the heavily loaded torsion strip could provide an almost perfect suspension that decouples the torsion balance from almost all extraneous influences except the gravitational torque of the sources masses.

3. The electrostatic torque transducer

As described in §1b, we balanced the gravitational torque with an electrostatic torque in the servo method. The torque was obtained directly in SI units from the change in total electrostatic energy, U, stored in the electrostatic actuator as a function of angle

$$U = \frac{1}{2}\underline{V}^t\underline{\underline{C}}\,\underline{V},\tag{3.1}$$

where $\underline{\underline{C}}$ represents the matrix of self and mutual capacitances and $\underline{V}$ is a vector of potential differences. In an electrostatically shielded volume, U can be written in terms of measurable cross-capacitances, C_{ij} [17]

$$U = \frac{1}{2}\sum_{i,j=1..3} C_{ij}(V_i - V_j)^2.\tag{3.2}$$

The torque can then be found from the derivative of equation (3.2), giving equation (1.1).

The idea of the electrostatic torque transducers came from the following observation regarding the capacitance between two cylinders moving in a plane perpendicular to their axes: if one cylinder approaches the other along a straight line such that the two cylinders will not touch, then there is obviously a maximum in capacitance at the point when the cylinders are at their smallest separation. This implies that the gradient of capacitance with respect to motion along the line must reach a maximum somewhere on either side of this peak. An analytical expression for the capacitance per unit length, C_{cc}, between two infinite cylinders of radius R_1 and R_2, with centres separated by distance D can be found in Smythe [18]:

$$C_{cc} = \frac{2\pi\varepsilon_0}{\cosh^{-1} u}, \tag{3.3a}$$

where

$$u^2 = \frac{D^2 - R_1^2 - R_2^2}{2R_1 R_2}. \tag{3.3b}$$

This was used to define the position of a cylindrical electrode relative to a test mass cylinder such that the change in capacitance with angle of motion of the mass was a maximum. In order to achieve a working control system, we clearly needed two electrodes. A two-dimensional finite-element program was written to investigate the cross-capacitances between the two puller electrodes and the test mass, C_{AC} and C_{BC}, and between both electrodes, C_{AB} themselves. The capacitance gradients, $dC_{AC}/d\theta$, $dC_{BC}/d\theta$, were found to be given to a good approximation by equations derived from equation (3.3). The electrostatic actuator was designed with two electrodes of radius 3 mm with a centre-to-centre distance of 9.4 mm and with a nominal minimum gap between the surfaces of the test masses and the electrodes of 1.5 mm. The nominal values of the capacitance gradients in the Mk II apparatus $dC_{AC}/d\theta$, $dC_{BC}/d\theta$ and $dC_{AB}/d\theta$ were 60.88, −61.74 and 0.33 pF rad^{-1}, respectively. This compares with values for $dC_{AC}/d\theta$ from the simple model of 70 pF rad^{-1}, with $dC_{AB}/d\theta$ being nominally zero.

The gap between the surfaces of the puller and the test mass in the Mk II experiment was 1.8 mm with the test masses having radii of 27.49 mm. Each set of four puller electrodes was electrically connected together using coaxial cables external to the vacuum can. The shielded cables within the vacuum can and the insulated ceramic mounts for the electrodes were confined to the bottom of the vacuum can where they were shielded by an aluminium plate that closely fitted around the base of the electrodes. This arrangement was a deliberate improvement on the Mk I apparatus where copper braid was used to provide a grounded shield around the insulation of the shielded cables in the vacuum can. All four pairs of puller electrodes were connected to ends of an aluminium 'cross', located underneath the false bottom of the vacuum can, that could be translated in two directions to centre the electrodes on the torsion balance.

An Andeen–Hagerling 2500A capacitance bridge was used to measure the three cross-capacitances at 1 kHz using the three-terminal method. It is important to note that this powerful method enables small capacitances, of order picofarads, between electrodes at the ends of long coaxial cables to be measured with ppm accuracy in terms of a standard capacitor. This is achieved by enclosing the electrodes in an electrostatic shield: one electrode is connected to the bridge drive voltage which has negligible output impedance (bridge 'hi') and the other is connected to bridge 'lo' which is at the potential of the bridge ground [19]. In this scheme, any currents that flow to the electrostatic shields owing to stray capacitances do not influence the bridge balance. Measurements of C_{AC}, for example, were made with the bridge 'lo' terminal attached to the 'A' set of electrodes and the bridge 'hi' was connected to the vacuum can, which was in turn electrically connected to the torsion balance. During this phase, electrodes B were connected to bridge ground. Capacitances, C_{BC}, were measured in a similar fashion. Capacitance C_{BC} was measured with the set A puller electrodes connected to bridge 'hi' and set B connected to bridge 'lo'. In this case, the vacuum can was connected to bridge ground. The standard 10 pF capacitance (model AH 11A) was calibrated at BIPM. The capacitance gradient was derived from measurements of capacitance and angle with the torsion balance freely swinging that were made before and after each data run.

During the phase of the experiment when the gravitational torques were being balanced by the electrostatic torques, each set of electrodes was connected via transformers to an Agilent 33120A function generator. The vacuum can, coaxial cable shields and the torsion balance were connected to ground. The servo signal, which was derived from the angular displacement readout of the autocollimator, was used to modulate the amplitude of the AC voltages produced by each generator. The generators were phase locked, and the servo voltage increased the amplitude of the output of one and reduced the amplitude of the other. We can write

$$V_A = (V_0 + v)\sin 2\pi ft, \tag{3.3c}$$

and

$$V_B = (V_0 - v)\sin 2\pi ft, \tag{3.3d}$$

where V_0 was 13 V and $f = 1$ kHz and the value of v, the drive voltage that balanced the gravitational torque, was about 10 V. The purpose of this scheme is to ensure that the torque was approximately linear in terms of the drive voltage v. The true RMS values of the AC voltages were measured using Fluke 5790A voltmeters that were calibrated at the Laboratoire National de Métrologie et d'Essais (LNE) leading to a fractional correction of -30 ppm to the value of G (see §11b). The potential drop across the cables between the meter and the electrodes amounted to less than 1 ppm of that measured.

The test masses are not expected to be at the same potential as the puller electrodes because of the contact potentials generated by the different metals comprising the torsion balance. During the early work using a DC servo system, we established that this contact potential was 24 mV. When this effect is included, the torque can be written

$$\tau_s = \frac{1}{2}\left\{\frac{dC_{AC}}{d\theta}\left\langle (V_A - \delta)^2\right\rangle + \frac{dC_{BC}}{d\theta}\left\langle (V_B + \delta)^2\right\rangle + \frac{dC_{AB}}{d\theta}\left\langle (V_A - V_B)^2\right\rangle\right\}, \tag{3.4a}$$

where the angle brackets indicate the time average is taken. Clearly with $V_A = V_B$, the cross terms in the angle brackets average to zero and the only remaining term is

$$\delta\tau_{s0} = \frac{\delta^2}{2}\left(\frac{dC_{AC}}{d\theta} + \frac{dC_{BC}}{d\theta}\right) \approx -2 \times 10^{-17}\,\text{N m}. \tag{3.4b}$$

In addition to this torque being entirely negligible, note that $\delta\tau_{s0}$ is a fixed offset and therefore cancels in the experimental procedure when the difference between the gravitational torques of alternate sign is found. Spatial variations in the potential (patch potentials) on the surfaces of the copper rods and the disc could give rise to further electrostatic forces that would have a stronger gap dependence than those modelled in the design of the torque actuator and so give rise to a contribution to the restoring torque. However, if present, this does not enter into the servo measurements and is accounted for by the measurement of the oscillation period in the Cavendish method.

Initially, we used a DC servo system but were unable to eliminate the possibility of frequency-dependent losses that could render the calibration of $dC_{ij}/d\theta$ at 1 kHz inconsistent with $dC_{ij}/d\theta$ at around 1 mHz. Biases in the calibration were such as to increase the apparent value of G in contradiction to that expected owing to loss mechanisms in surface films on the electrodes [20]. However, it can be shown that a grounded lossy dielectric located in the electric field will add, in parallel, a frequency-dependent capacitance such that the measurement of $dC_{ij}/d\theta$ at high frequency overestimates the calibration constant. We encountered the possibility of such a bias in our early work by noting that the Q of the torsion balance was halved on application of 2 kV DC to the electrodes. We later identified a coaxial cable whose electrostatic shield was not grounded and whose insulating cover was exposed thus affecting the fringing field of a pair of electrodes. We suggested that a similar effect may have been present in the PTB measurement, because, in their experiment, the calibration and measurement frequencies differed by orders of magnitude, as was the case in our preliminary work. Such problems are eliminated by using an AC servo. Supplementary investigations [21] by the PTB team discovered (at the instigation of one of us, C.C.S.) that a term in the electrostatic energy had not been measured. Although the

torsion balance itself had been dismantled, PTB was able to measure this extra cross capacitance and concluded that its inclusion would reduce the final value of *G* by 0.71%. This must therefore be considered as the most significant systematic bias in the PTB measurement.

4. The test and source masses

The size and scale of the whole apparatus was set by the initial decision to limit the weight of the source masses to about 11 kg, the maximum that one of us (T.J.Q.) considered reasonable to manipulate by hand. The second important decision was to make both source and test masses in the form of right circular cylinders from Cu–0.7% Te free-machining alloy susceptible to manufacture in the BIPM workshop and resulting in small magnetic contamination from machining (see §10). Both test and source masses were made with their heights equal to their diameters, 55 and 118 mm, respectively, in order to produce radial gravitational fields that were as large as possible. At the separation between the source and test masses (about 107 mm), the magnitude of the gravitational field due to the source masses corresponded to about 90% of that due to a sphere of the same mass. For the Mk II apparatus, new test masses were made, and the source masses were cut down to 115 mm in height. Calculations of their individual gravitational fields assuming they were spherical differ by about 10% from a calculation treating them as cylinders. Although it was not necessary to make the four source masses and the four test masses of exactly the same size, in fact they were quite close in dimension and in mass. The masses in the Mk II were about 1.2 and 11.2 kg, respectively, for each of the test and source masses, similar to Mk I.

A critical parameter in all measurements of *G* is the uniformity of density of the attracting masses. Cu–0.7 Te is an alloy that can be cast in molten form into billets which are then swaged to obtain a material free of voids. However, as we discovered, this hot working of the material leads to stresses and associated small density gradients. For both source and test masses, we measured the density inhomogeneities by hydrostatic weighing of samples cut from the original billet and, for the source masses, by determining their centres of gravity with respect to their geometrical axis from measurements of their dynamic-equilibrium position and period of free oscillation when supported on an air bearing. We found that the density varied linearly across the diameter of the source masses. The density at the centre differed from that at the perimeter by an amount $\Delta\rho_0$ and this increased from about one to two parts in 10^4 along the length of the billet. Such a transverse linear density gradient was not what we expected and results in a $\cos\phi$ dependence of density in each source mass, where ϕ is an angle measured in the plane perpendicular to the nominal symmetry axis of the cylinders. The inner mass multipole moments, e.g. q_{11}, were therefore present in the source masses that were not accounted for in the basic calculation of the gravitational coupling between the source, test masses and torsion balance. A more detailed analysis (following the method given by D'Urso & Adelberger [22]) shows that these inner moments interact with outer moments, e.g. Q_{22}, of the test masses. These moments can in turn be calculated from the inner moments of the test masses using results taken from Trenkel & Speake [23]. This calculation shows that the torque between the two masses, whose centres are a distance *a* apart (approx. 107 mm) has an extra term which is given to first order as

$$\frac{\Delta\Gamma}{\Gamma} = \frac{5}{6}\frac{R_s}{a}\frac{\Delta\rho_0}{\rho_0}\cos\phi_0\cos\phi, \tag{4.1}$$

where R_s is the radius of the source mass, ϕ is the orientation of the q_{11} multipole and ϕ_0 is the angle joining the centres of the source mass and torsion balance which is 21.5° for a source mass offset of 18.9°. Using the measured density inhomogeneities, this gave the maximum fractional error of about 90 ppm for one source mass. When the torques, owing to all source and mass pairs, were summed, this reduced to −32, −0.4 and 36 ppm, depending on the orientation of the source masses. In the analysis of the results from the Mk II experiment, the effect of the mass inhomogeneities was calculated numerically (see §9) to be −22, 2 and 25 ppm. Thus, in any case, the errors of the torques at the three angular positions of the source masses, 120° apart, average

almost to zero as expected. In the Mk II experiment, the source masses were in the configuration such that the inhomogeneity led to correction of -2 ppm for the Cavendish and -22 ppm for the servo data that were included in the calculation of the torques. A linear axial variation amounting to 100 ppm over the length of each source mass was also found by hydrostatic weighing. This introduced an axial shift in the centres of mass of about 1 μm, which in turn produced a negligible change in torque. The source masses used in both experiments were the same except that for the Mk II experiment a 3 mm slice was removed from one end in order to allow new 'V' grooves to be cut. The density inhomogeneity of each mass was then rechecked using the air bearing, the difference being negligible. In addition, X-ray examination showed the absence of axial voids (the only inhomogeneity in the source masses that would not have been detected by these and earlier tests) with diameters greater than 2 mm (1 ppm). Such axial voids in a swaged billet otherwise free of voids would in any case have been most unlikely.

The far smaller billet from which the test masses were cut showed no azimuthal dependency within the uncertainty of our measurements. The accuracy of the density measurements was limited to about 5 ppm but, owing to the shape of the samples used, linear variations of 9 ppm could not be ruled out. Using equation (4.1) to calculate the analogous torque error for the test mass inhomogeneity, we find a maximum fractional change in torque for a single mass pair of about 1.7 ppm. We would expect that, when summed over all pairs, this would be reduced to less than 1 ppm. This was considered negligible and was not included in the uncertainty budgets.

The variation of density across the radius would shift the centre of gravity of the test masses, and this would produce an error in the calculation of the moments of inertia. If we have a density gradient across the diameter of a cylinder with $\Delta\rho = \Delta\rho_0(r/r_t)\cos\phi$, where r and r_t are the radial distance from the axis of symmetry and the radius of the test mass, respectively, the shift in the centre of mass of the cylinder can be calculated as $\delta r = (\Delta\rho_0/\rho)(r_t/4)$. Assuming a random orientation of the masses, the first-order fractional change in the moment of inertia of the torsion balance is given by $\Delta I/I \approx \delta r/(\sqrt{2}d)$, where d is the average radial distance of the centre of the masses to the axis of rotation. This amounts to a change of much less than 1 ppm in the moment of inertia which is negligible. This systematic effect, if present, would show up differently in the Cavendish and servo methods. The experimental measurement of the moment of inertia, albeit with an uncertainty somewhat larger than 1 ppm, confirmed that there was no significant error in the calculation of the inertia from this or any other source. The uncertainty in the calculation of the moment of inertia was based on dimensional metrology as described in §8.

The kinematic mounting of the source masses on the carousel was by means of three 'V'-grooves cut in the base of the masses at 120° close to the periphery and three cones in the carousel in which 5 mm diameter phosphor bronze balls were placed. This provided a reproducible positioning of the 11 kg masses after multiple placing and removals. This is discussed in §5.

5. Dimensional metrology

Dimensional metrology is another key part of any G experiment. Uncertainties owing to errors in dimensional metrology were calculated using an approximate expression for Γ that was derived from a multipole expansion assuming all the masses to be points (see §11) [16]

$$\Gamma = 35Mm\frac{r^4}{R^5}\sin 4\theta, \tag{5.1}$$

where M and m are the nominal source and test mass values, respectively, r and R are the nominal values of the radial distances of the source and test masses from the torsion strip rotation axis, respectively. Equation (5.1) gives an approximate value for the amplitude (i.e. half the peak–peak) torque in terms of the position of the source masses, θ, with $\theta = 0$ corresponding to the source and test masses at their closest position. This expression agrees with the final computed value within

about 1%. Overall scaling errors common to both test and source mass positions lead to errors in G proportional to $\Delta l/l$, where l is the distance from the balance axis. However, uncorrelated errors in the measurement of the relative positions of the test masses contribute (in quadrature) as $4\Delta l/l$ and for the test masses as $5\Delta l/l$ and can thus lead to much larger errors in G.

We chose to mount the apparatus on the base of a CMM so as to give the best possible opportunity of attaining accurate dimensional metrology. Two different CMMs were used, for the Mk I a DEA Swift and for the Mk II a Brown and Sharpe Mistral. In both cases, the CMMs incorporated man-made marble base plates onto which the experiment was assembled. A spherical ruby stylus was attached to a mobile carriage, manufactured almost entirely from an aluminium alloy for lightness and rigidity, running on air bearings constructed directly in the marble surface of the table. When not being used for metrology, the carriage was parked at the farther end of the marble table. In the Mk I experiment, the instrument was calibrated by the manufacturer on site and subsequently checked by means of end gauges calibrated by the LNE. In the Mk II experiment, following a change observed in the original calibration of the manufacturer, the x- and y-scales were recalibrated by us using a laser interferometer. The uncertainty in the new calibration was established in two steps: first the x- and y-scales of the CMM were calibrated using the laser interferometer and second by using 300 and 500 mm gauges placed at various orientations across and on top of the source masses and also, for the 300 mm gauges, placed alongside the source masses at their mid height. A total of 14 measurements of the gauges were made. Taking all the measurements together, the average difference between the gauge lengths (corrected to the temperature of the measurement) and the corrected CMM readings was $+0.38\,\mu$m with a standard deviation of $0.9\,\mu$m which for $n = 14$ gives a standard deviation of the mean of $0.25\,\mu$m. From this, we estimated the uncertainty of the calibration of the CMM to be $0.4\,\mu$m, i.e. the common errors that affect both test and source mass positions can be taken to be about $0.4\,\mu$m. This is equivalent to type B uncertainties of 3 ppm in respect of the test masses and 2 ppm in respect of the source masses.

The type A uncertainties in the source mass coordinates were established by sets of measurements of the relative source mass positions in position A at $+18.898°$ from zero, position B is at $-18.898°$. Each value for x and y of the centre of each source mass came from a set of eleven points measured around the circumference, each mass being measured seven times. The average standard deviation of the seven measurements about its average was $0.5\,\mu$m, a figure confirmed by repeats of this procedure. On the basis of these measurements, the six different distances between the four masses, 1–4; 1–3; 1–2; 2–3; 2–4; and 3–4, were calculated. The average difference between each of these distances (which were either about 302 or 428 mm) over a period of about one week was $0.52\,\mu$m with a standard deviation of $0.16\,\mu$m. The 300 mm gauge block was also placed at the four possible positions across the source masses 2–3; 2–1; 1–4; and 4–3. The difference between the gauge block measurements measured at the beginning and at the end of this week was $0.5\,\mu$m with a standard deviation of $0.2\,\mu$m. From these data, we estimate the type A uncertainty in the source mass positions as $0.5\,\mu$m, equivalent to an uncertainty in the measured value of G of 12 ppm. Similar type A uncertainties were obtained for the test mass coordinates to a type A uncertainty of 17 ppm in the value of G.

The uncertainty in the radii of the source masses (about 120 mm) was established from seven sets of measurements made at the three orientations, A, B and C, from January to March 2007. The standard deviation of the seven values of radius about the average for each source mass was $0.6\,\mu$m for masses 1 and 3, $0.5\,\mu$m for mass 2 and $0.2\,\mu$m for mass 4. The standard deviation of the means becomes 0.2, 0.2 and $0.1\,\mu$m, respectively. Dividing the set of seven measurements into three groups, those at orientation A, B and C, the average radius of the set of four masses in the three orientations was identical at 58.9876 mm. This result demonstrates both the reproducibility of the measurements and, more importantly, agreement to within $0.1\,\mu$m for all three orientations of the source masses.

The coordinates of the centres of both the test and source masses were obtained using the CMM software, which calculates the centre from sets of measurements around the circumference. This software was checked by an independent calculation, which also allowed the CMM x- and

y-scale corrections to be included in all subsequent measurements. The long-term reproducibility of the measurements was consistent with the estimated uncertainties, namely a few tenths of a micrometre.

At the end of the Mk I work, in 2001, the last measurement was of the relative positions of the source masses on the carousel. The carousel was then removed to the new laboratory where the Mk II work was due to begin and placed on the base of the new CMM and the source masses replaced. A new CMM had been purchased for internal operational reasons related to equipping the BIPM mechanical workshop with a CMM. Measurements of the relative positions of the source masses measured by the two CMM were found to agree to about $1\,\mu m$. This provided a good comparison between the dimensional metrology in the two experiments. It also illustrated our experience over all the years of the two experiments that removing and replacing the source masses on their kinematic mounts resulted in a reproducibility of relative position of 1 or $2\,\mu m$. It was sometime after this that the calibration of the new CMM was found to have changed, which led us to the calibration with the laser interferometer. Subsequent measurements against end gauges showed no further changes.

6. Angle measurement

Angle measurement intervenes in both the servo and Cavendish methods. In the servo method, it is necessary to calibrate the electrostatic servo by determining $dC/d\theta$ for each of the pairs of electrodes and in the Cavendish method the deflection of the torsion balance must be measured. Two different autocollimators were used, an Elcomat 2000 for the Mk I and an Elcomat HR for the Mk II, both from the Möller–Wedel Company. Both were calibrated by the PTB, but in the case of the Elcomat HR, two calibrations were made in 2003 and 2006. The performance of the Elcomat HR was the subject of an extensive study by the PTB. In the first instance using the mirror attached to the torsion balance, and in the second instance the calibration was undertaken with a mirror supplied by the PTB. In both calibrations, the optical path, apertures and windows were those used in the *G* experiment. The electronics had been modified by the manufacturer to enable precise timing to be made of the angle data sent from the autocollimator to the controlling computer of the experiment and thus correctly related to the time signals from the atomic clock which was the time reference. The PTB calibration gave the deviations from nominal over a range of ± 100 as at 1 as intervals with a resolution of 0.1 mas. The deviations did not exceed 3 mas over about 40 as near the centre of the range within which almost all the measurements were made; note that the *G* deflection amounted to a total of 31 as. The absolute type B uncertainty of the calibration, common to both servo and Cavendish measurements, was 1.5 mas with relative errors within this range being at the level of the resolution.

In the Mk II experiment, the angle was measured by a single reflection of the autocollimator beam from a mirror mounted near the axis of the torsion balance. This is in contrast to the Mk I experiment in which the torsion balance was equipped with a set of mirrors that multiplied the angle by a factor of 6. Comparisons between deflection measurements made using the multiplying optics and directly showed agreement well within the standard deviation of the mean of the values obtained directly, but these were of course some six times larger than those obtained with the multiplying optics. After the Mk I work was completed, there was some concern about the effects of non-flatness of these multiplying mirrors that made us decide to use a simple single reflection system for the Mk II. As was the case for many of the changes to the Mk I experiment, this modification was not motivated by any real hard evidence for the presence of a systematic effect in the Mk I experiment, but more by the desire to eliminate any possible source of systematic uncertainty that remained undiagnosed in the first experiment.

The disadvantage of course is that the six times gain in sensitivity is lost although this was compensated by the improved resolution and accuracy of the Elcomat HR.

There is a straightforward correction that has to be applied to the angle measured by the autocollimator owing to the refractive indices being that of air and vacuum on either side of

the window in the vacuum can. The true angle, ψ, can be written in terms of the measured angle, ψ_m, as

$$\psi = \frac{n_{air}}{n_{vac}} \psi_m, \tag{6.1}$$

where we use $n_{air} = 1.000271$ (NIST Engineering Metrology Toolbox; http://emtoolbox.nist.gov/Wavelength/Edlen.asp).

7. Timing

The period of oscillation was determined by fitting, using a nonlinear least-squares algorithm, oscillation amplitude and time pairs to the equation of a damped harmonic oscillator with a constant offset. The timing of the data pairs in the Mk II experiment was referenced to a 10 MHz signal from an atomic frequency standard in the BIPM time section. The corresponding uncertainty in G was a nominal 1 ppm. In the Mk I experiment, a much larger uncertainty had been given, 35 ppm, because of doubts as to the reliability of the link to the then atomic frequency standard of the BIPM.

8. Calculation of the moment of inertia of the torsion balance

The moment of inertia, I, of the torsion balance about its axis of rotation was both calculated and measured. Because it enters directly into the calculation of G in the Cavendish method, its uncertainty must be equal to or less than the uncertainty sought in G. The torsion balance assembly consists of an aluminium alloy disc, the cylindrical copper–tellurium test masses, the copper–beryllium clamping base, the rectangular cross-section copper beryllium clamping block that holds the torsion strip, an aluminium cylindrical tower and an aluminium tube with lugs for the attachment of the mirror support plates and the mirrors. The assembly was held together by 32 M3 screws and eight M6 screws (for the torsion strip clamp). In view of the complexity of the torsion balance, see figures 1, 2 and 5, the calculation of its moment of inertia posed a considerable challenge. This was easier for the Mk II apparatus, because every component had been made using a computer-aided design program and constructed on numerically controlled machines in the BIPM workshop. The relative positions and dimensions of every component were, in principle, known. Nevertheless, manual checks were carried out with the CMM and a micrometer to verify the most important dimensions. These included the measurement with the CMM of the position and dimension of every hole and cut-away seating for the test masses in the torsion disc as well as multiple measurements of the thickness of the disc using the micrometer. It was discovered that in the final machining of the 8 mm thick disc, the milling machine had removed about 10 µm too much over about one-third of the disc on one side. The uneven thickness of the torsion disc was modelled as a superposition of a uniform disc with the mean thickness with associated holes and a disc of varying thickness and its associated cylindrical holes. Note that the torsion discs for the Mk I apparatus was manufactured from duralumin, whereas that for the Mk II experiment was made from AU 4G aluminium alloy.

The moment of inertia of the torsion balance was calculated using both the primitive geometrical shapes described above and computer-aided design packages together with the measured masses of the components. The torsion disc without the test masses, modelled as a nominal uniform disc, comprised approximately 9% of the total inertia. The sum of the other components on the torsion balance including the torsion strip clamp, the mirror assembly, screws, etc., amounted to about 0.79%. The uncertainty, δI_i, in each component of the moment of inertia, I, is computed as

$$\left(\frac{\delta I}{I}\right)_i = \sqrt{\left(\frac{\delta d_i}{d_i}\right)^2 + \left(\frac{\delta m_i}{m_i}\right)^2}, \tag{8.1}$$

where d_i and δd_i are the radius of gyration of each component and its uncertainty and m_i and δm_i are the mass of the component and its weighing uncertainty. The final uncertainty in the
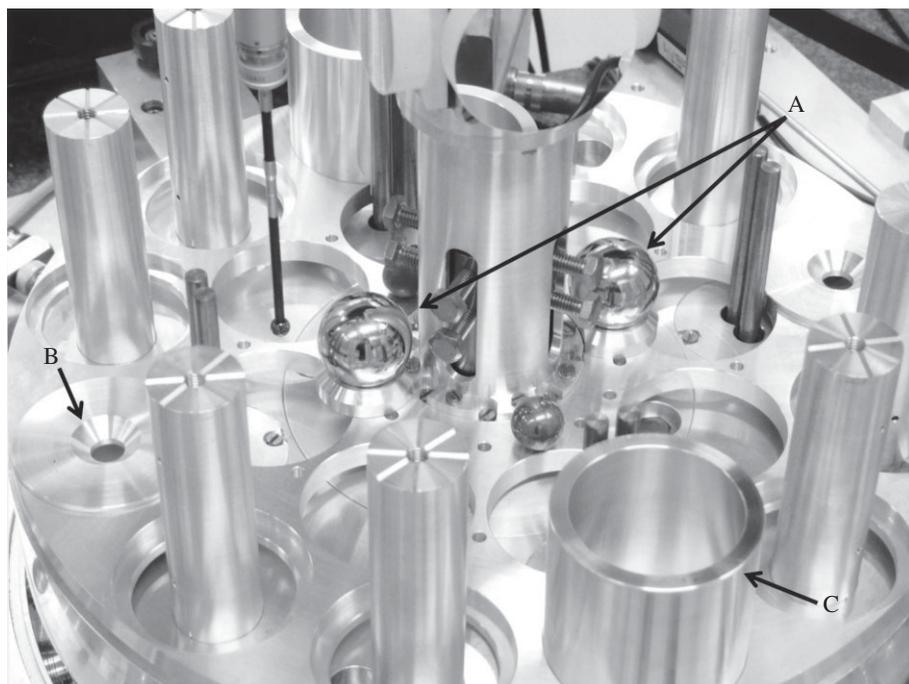
Figure 5. The torsion balance illustrating the configuration in preparation for the measurement of moment of inertia showing (A) the two stainless steel balls in place in their inner position, (B) the outer position of one of the balls and (C) one of the two aluminium cylinders occupying the place of two of the test masses necessary for the electrostatic servo control of the torsion balance. The CMM probe for measuring the position of the balls is visible. The whole of the top assembly has to be removed for the measurement of the position of the balls but has to be in place for the successive measurement of the period with the balls in their inner and outer positions.

moment of inertia of the torsion balance, not including the test masses, amounted to 11 ppm of the total moment of inertia. The uncertainty in the moment of inertia of the test masses alone amounted to 8 ppm.

The moment of inertia of the torsion balance disc assembly in the Mk II apparatus was checked by measurement. A scheme was devised in which a pair of identical stainless steel spheres of known mass (about 100 g) could be placed first near the outer edge of the disc and second close to its central pillar. This was done at the end of the whole experiment when the test masses had been removed from the torsion balance. In order to mount the stainless steel spheres and to provide electrodes for the servo control needed to manipulate the torsion balance in vacuum, a number of small aluminium pieces had to be made to support the spheres and to replace two of the test masses as electrodes (figure 5). Their mass and shapes were taken into account in the calculation of the inertia. From measurement of the periods of free oscillation of the balance with the spheres in these two carefully measured positions, we could determine the change in moment of inertia of the disc assembly. By assuming that the restoring torque remained unchanged in the two configurations the inertia of the disc assembly could be determined. From this, a value for the total inertia was calculated having an estimated uncertainty of 25 ppm. It differed from the calculated value by only 9 ppm. In the Mk I experiment, the moment of inertia of the torsion balance was simply calculated. The value of the total moment of inertia of the Mk II torsion balance is

$$I = 0.0762332(10) \ \text{kg m}^2, \tag{8.2}$$

with an uncertainty of 13 ppm.

9. Calculation of the torque

For the purposes of the calculation of the torque factors coupling the torsion balance assembly and the source mass/carousel assembly, Γ_s and Γ_c for the servo and Cavendish methods, respectively, the experiment can be considered to comprise a set of *test* objects mounted on the torsion balance. These are attracted by a set of *source* objects mounted on the carousel. Both source and test objects are defined to be either cylinders, with vertical axes, or simple points.

The *test cylinders* comprised the four test masses themselves, the torsion balance disc of uniform thickness and its array of cylindrical holes in the disc of varying thickness. The torsion strip clamping block, the tower supporting the mirror mounting tube and the mirror mounting block also had components that were modelled as test cylinders.

The *test points* comprised the 'overlap' regions, the points that generate the uneven part of the disc surface, the trim masses (phosphor bronze balls, two of mass 1.49 g and one of 19.17 g used to finely tune the horizontality of the disc), the screws and various non-cylindrical parts of the mirror column, the strip clamping block, the mirror mounting tube, the mirror mounting plates and the mirrors themselves. The 'overlap' regions were adjacent to each of the four test masses and were created by the partial overlap between the outer and first inner array of holes. This design allowed the electrostatic puller electrodes to be positioned adjacent to the source masses without being obstructed by the torsion disc.

The *source cylinders* comprised the copper–tellurium source masses which are modelled as geometrically perfect cylinders of uniform density.

The *source points* comprised the components of the kinematic mounts: six grooves in each source mass, three balls and three grooved in the aluminium alloy carousel for each source mass.

The total torque was modelled as the sum of the following components:

— the attraction between the test cylinders and uniform cylindrical source masses. The torque between the source cylinders and the four test masses is the largest contribution and this is calculated by numerical integration over the test mass volumes of the semi-analytical expression [24] for the gravitational field generated by the source masses. We used numerical algorithm group routines to calculate the elliptic integrals required in [24]. The torques owing to the other cylinders are calculated using a multipole expansion (referred to in the 2001 paper but not published);

— the attraction between the test cylinders and the source points. This torque is calculated using the semi-analytical result in [24] to calculate the field owing to the test cylinders at the source points. This amounted to +1 ppm of the total torque;

— the attraction between the test points and the source cylinders. This is calculated again using the result in [24] (+150 ppm); and

— the correction owing to a linear density gradient across the source masses. We calculate the attraction by numerical integration between the inhomogeneous part of the source masses and the test masses assuming the measured linear density gradient for each source mass. This amounted to a reduction in Γ_s of 22 ppm and an increase in Γ_c of 2 ppm.

The coordinates, r_i, of all the source and test components were collected into data files. The files also contained, in the case of cylinders, radius, height and density, or in the case of points, masses, for each source and test object. The density of the test masses was calculated based on the 'true mass' which is the density that would be deduced from a weighing in vacuum. The density of the source masses was calculated from the 'effective mass'. This density would also be deduced from the true mass but less the density of air at the nominal standard conditions of our ambient atmospheric pressure, temperature and air composition. These data were used to compute both the moment of inertia and the gravitational torque factors Γ. The torque was calculated in the usual way using

$$\Gamma_z = \sum_{ij} X_i \times F_{Xj}, \tag{9.1a}$$

where

$$F_{Xj} = \frac{X_j - X_i}{|r_j - r_i|^3} \tag{9.1b}$$

and X_i and X_j are the positions of test and source object in the horizontal x, y plane, respectively. This expression, in terms of the pure forces produced by the source objects, is valid provided that the test objects are cylindrically symmetric about their individual centres of mass. Higher-order terms owing to quadrupole moments (q_{22}, for example) of the individual components of the torsion balance assembly are negligible.

Consistency between the three methods of calculating the Newtonian torques (numerical integration, the expression derived from [24] and the multipole expansion) was checked by direct calculation.

In the initial Cavendish experiment, the offset between the average position of the source masses and the test masses was established by rotating the carousel through angles $+\theta$ and $-\theta$ and ensuring that the magnitude of the torques was the same. The rotation angle was then varied between 18° and 20° with a peak in the torque difference occurring at $\theta_M = 18.898°$. In all subsequent measurements, the offset angle was found in a similar fashion, and the source masses rotated about this offset by $\pm 18.898°$. The calculations showed that the offset angle differed by 6.30 mrad between the servo and Cavendish configurations of the source masses and this was in good agreement with the difference in the mean angular positions of the masses as measured by the CMM (6.31 mrad). Calculation also showed that, owing to asymmetries in the mass distributions, the peak torque difference was a weak function of both the offset and the amplitude. Finding the absolute peak would have entailed adjustment of the offset at a level of much better than 1 ppm which was not possible. However, given the amplitude of θ_M, the offset and the peak torque is defined. The accuracy of the angle measured was estimated to be about 0.001° (given by the number of stepper motor steps required to make a complete rotation) and the peak torque could be calculated with negligible uncertainty.

The values of the servo and Cavendish torque coefficients were

$$\Gamma_s = 471.5875 \, \text{kg}^2 \, \text{m}^{-1} \tag{9.2a}$$

and

$$\Gamma_c = 471.6511 \, \text{kg}^2 \, \text{m}^{-1}. \tag{9.2b}$$

The two values differ because of the shift in position of the source masses when they were rotated to be in different positions in their kinematic mounts. The change in the orientation of the density gradients produces a smaller difference.

10. Possible magnetic interactions between the source and test masses

An experiment was carried out in which the torque was measured when the source masses were removed from the carousel leaving only the three 5 mm supporting balls in the V-grooves below each mass. The resulting signal, which amounted to 65 ppm of the total G signal with the source masses present, was consistent with expectations based solely on calculated gravitational interactions between the balls and the conical holes in the carousel with the torsion balance. Therefore, we focus on possible magnetic interactions that might influence the measurements when the position of the source masses is changed relative to the test masses.

The design of the BIPM G experiment results in a large signal torque between the source and test masses. This can be demonstrated simply by a naive calculation of the gravitational attraction between two osculating Cu–0.7% Te spheres, one of which is 11.2 kg and the other 1.16 kg, resulting in an attractive force of about 90 nN. To compare with, say, the magnetic force between the spheres owing to their magnetic moments induced by the Earth's magnetic field, a similar calculation can be made assuming that the line of centres of the osculating spheres is aligned in

the field, which is about $40\,\mathrm{A\,m^{-1}}$ at Sèvres. We measured the volume magnetic susceptibility of the Cu–0.7% Te alloy to be essentially equivalent to that of pure copper ($\chi = -9 \times 10^{-6}$), which results in a force that is nine orders of magnitude smaller than the gravitational attraction. Note, however, that if both spheres had been made of high-quality austenitic stainless steel ($\chi \approx 0.003$), then the magnetic force would be only four orders of magnitude less than the gravitational force and a more searching analysis would have been required. In this worst-case model, an extraneous magnetic field strength of about $3.3\,\mathrm{kA\,m^{-1}}$ would have been required to produce an erroneous G signal of order 1×10^{-5} in our apparatus. Field strengths of this size owing to nearby equipment, such as the CMM, were not present. As noted above, a different CMM was used for our previous work, and the large metallic parts of both were made of aluminium alloy.

Remanent magnetization in various pieces of the apparatus might also lead to significant torques between the torsion balance and the source masses. We verified that the largest pieces, made of Cu–0.7% Te and aluminium alloy, were magnetically 'clean'. We also screened smaller pieces of the torsion balance made of a variety of different materials in order to ensure handbook magnetic susceptibilities and the absence of serious remanent magnetism. Note that cold-working, such as the cutting of threads in screws during their manufacture, can degrade the magnetic properties of some 'non-magnetic' alloys. We found many examples of this and rejected the pieces. In addition, the use of steel cutting tools during the shaping of copper pieces may leave a ferromagnetic deposit on soft metals which would need to be removed by acid etch. The Cu–Te alloy did not have this problem, unlike oxygen-free high thermal conductivity (OFHC) copper.

In the final version of our apparatus, the torsion strip was suspended from crossed knives forming a universal joint in order that the test mass assembly, including the aluminium disc, would hang plumb. The pendulum modes of the strip were suppressed by a magnetic damper installed above the crossed knives. Acid-etched OFHC copper was used in the damper. The aluminium construction of the moving structure of both CMMs would have resulted in no significant magnetic interactions with either the source masses or torsion balance.

11. Uncertainty calculations for the value of G

(a) Uncertainty in the torque due to mass positions

We break down the uncertainty in the positions of the source and test masses into random and systematic components. Using the gauge blocks, we established a type B uncertainty for the source and test mass positions of $0.5\,\mu\mathrm{m}$, and we find fractional uncertainties for $\delta R_b/R$ and $\delta r_b/r$ of 2 and 3 ppm. The type B uncertainties owing to the source mass and test mass positions affect the servo and the Cavendish measurements in different proportions as discussed below. An uncertainty owing to the differences between the times when the temperature measurements and the dimensional metrology are made is added in quadrature to the type A uncertainties.

We use the simple model given in equation (5.1) to calculate the uncertainties in the torque owing to the positioning uncertainties. The test and source mass arrangements are assumed to have a perfect fourfold symmetry and we assume that the centres of the source and test masses are in the same horizontal plane. The simple model gives a peak value for the torque at $22.5°$ (rather than approx. $19°$) which agrees with the full calculation to within a few per cent.

We can estimate the uncertainties in Γ using the uncertainties in the mass positions described above

$$\frac{\delta\Gamma}{\Gamma} = \frac{\delta m}{m} + \frac{\delta M}{M} + \frac{4\delta r}{r} - \frac{5\delta R}{R}. \tag{11.1}$$

We can separate the systematic and random contributions for the position uncertainties for a particular measurement as

$$\frac{\delta\Gamma}{\Gamma} = \frac{\delta m}{m} + \frac{\delta M}{M} + \delta\alpha + 4\frac{\delta r_a}{r} - 5\frac{\delta R_a}{R}, \tag{11.2a}$$

where, from §5, $\delta r_a = \delta R_a = 0.5\,\mu\text{m}$. The quantity $\delta \alpha$ corresponds to the change in torque owing to an overall change in length scale. For the servo measurement

$$\delta \alpha_s = 4 \frac{\delta r_b}{r} - 5 \frac{\delta R_b}{R}, \tag{11.2b}$$

which amounts to 4 ppm for $\delta r_b = \delta R_b = 0.4\,\mu\text{m}$. As shown below, for the Cavendish measurement

$$\delta \alpha_c = 2 \frac{\delta r_b}{r} - 5 \frac{\delta R_b}{R} = -3\,\text{ppm}. \tag{11.2c}$$

Note that the type A uncertainty for the test masses positions produces a correlated uncertainty in both methods, so we do not distinguish between test mass type A coordinate uncertainties for the two methods. If we assume a temperature variation of 0.1 K, then this will give a torque variation that will scale as $\delta \alpha$ for both methods. We can write $\delta \alpha_{sT} = 2\,\text{ppm}$ and $\delta \alpha_{cT} = 6.9\,\text{ppm}$ for aluminium alloy.[2] These uncertainties are considered to be random and uncorrelated between the two methods.

(b) The servo method

In the servo method, the gravitational torque can be calculated in terms of the measured capacitance gradients and the measured differences in RMS voltages as described in §3

$$\tau_s = \frac{(1 + \delta_V)}{n_{\text{air}}} \frac{1}{2} \left\{ \frac{\mathrm{d}C_{AC}}{\mathrm{d}\theta} \Delta \langle V_A^2 \rangle + \frac{\mathrm{d}C_{BC}}{\mathrm{d}\theta} \Delta \langle V_B^2 \rangle + \frac{\mathrm{d}C_{AB}}{\mathrm{d}\theta} \Delta \left\langle (V_A - V_B)^2 \right\rangle \right\}, \tag{11.3}$$

where $\delta_V = -30\,\text{ppm}$ is the calibration correction for the AC voltmeters (given in §3), and the refractive index corrects the autocollimator angle measured in air to that in vacuum as described in §6.

For the purposes of modelling the uncertainties, we can write

$$\tau_s \approx \beta \Delta V^2, \tag{11.4}$$

with $\beta \sim \mathrm{d}C_{AC}/\mathrm{d}\theta$.

The uncertainty in the value of G measured by the servo method is then

$$\frac{\delta G_s}{G} = \frac{\delta \beta}{\beta} + 2 \frac{\delta \Delta V}{V} - \left(\frac{\delta M}{M} + \frac{\delta m}{m} + 4 \frac{\delta r_a}{r} - 5 \frac{\delta R_{as}}{R} + \delta \alpha_s + \delta \alpha_{sT} \right), \tag{11.5}$$

where we have identified the random uncertainty on the source mass coordinates in the servo measurement, δR_{as}.

Further, the capacitance gradient has a systematic component and a statistical contribution: there are uncertainties due to the absolute accuracy of the angle and capacitance changes over the range of the calibration and there is the statistical uncertainty, $\delta \beta_a$, from measurement noise:

$$\frac{\delta \beta}{\beta} = \frac{\delta \Delta C}{\Delta C} - \frac{\delta \Delta \theta}{\Delta \theta} + \frac{\delta \beta_a}{\beta}. \tag{11.6a}$$

So we can write

$$\frac{\delta G_s}{G} = \frac{\delta \Delta C}{\Delta C} - \frac{\delta \Delta \theta}{\Delta \theta} + \frac{\delta \beta_a}{\beta} + 2 \frac{\delta \Delta V}{V} - \left(\frac{\delta M}{M} + \frac{\delta m}{m} + 4 \frac{\delta r_a}{r} - 5 \frac{\delta R_{as}}{R} + \delta \alpha_s + \delta \alpha_{sT} \right). \tag{11.6b}$$

In the experimental procedure, the capacitance gradient β that was used to calculate the torques from the voltages was the mean of the capacitance gradients measured before and after the torque measurements. During a sequence of torque measurements, the dimensional metrology and all

---

[2]In [2], the thermal uncertainty was added in quadrature to the type B uncertainty in dimensions and this decreases the correlation (more negative) and gives rise to a difference in the final uncertainty of 2 ppm in the results given here.

type B uncertainties are essentially constant, and we determine the value of G from the differences in gravitational torques acting on the torsion balance so we can write

$$\delta\tau_s = \delta(\beta\Delta V^2) + \delta n, \tag{11.7a}$$

where δn is a random change in torque produced by ground vibrations for example. However, any random change in the value of β that occurs that is within the bandwidth of the servo will be balanced by a change in the applied servo voltages

$$\delta\tau_s = 0 = \delta\beta_a\Delta V^2 + \beta\delta\Delta V^2 + \delta n. \tag{11.7b}$$

The type A uncertainties in β become indistinguishable from the noise torques and so we can define a general noise torque

$$\delta n' = \beta\delta\Delta V^2 = -\delta\beta_a\Delta V^2 - \delta n. \tag{11.7c}$$

The type A uncertainty in the capacitance gradient can then be considered to be part of the statistical noise in the torque measurements with $\delta\tau_s = -\delta\beta_a\Delta V^2 - \delta n$. The standard deviation of the mean of the 10 servo measurements was 30 ppm and this was consistent with the standard deviations of the individual measured torques, which themselves included the recalibration of the β values between each torque sequence. The standard deviation of the mean of the 10 torque sequences measured by the Cavendish method was 19 ppm. We can interpret this difference to be owing to variations in β. We found that the standard deviations of the calibration constants measured between each torque sequence were far too large to be consistent with the variance of the torque data, and we attribute this to high-frequency electrical noise affecting the capacitance bridge which evidently was averaged out. Finally, we have the following equation describing the uncertainties in the servo measurement:

$$\frac{\delta G_s}{G} = -\frac{\delta M}{M} - \frac{\delta m}{m} - 4\frac{\delta r_a}{r} + 5\frac{\delta R_{as}}{R} - \delta\alpha_s - \delta\alpha_{sT} - \frac{\delta\Delta\theta}{\Delta\theta} + \frac{\delta\Delta C}{\Delta C} + 2\frac{\delta\Delta V}{V} + \frac{\delta\tau_s}{\tau_s}. \tag{11.7d}$$

(c) The Cavendish method

We calculate a value for G for this method using equations (1.2) and (2.6b)

$$\tau_c = n_{air}k_r(\omega_m)\Delta\theta_c, \tag{11.8}$$

where $k_r(\omega_m)$ is the angular stiffness of the torsion balance at the frequency of the measurements. The angle through which the torsion balance moves is $\Delta\theta_c$. The refractive index correction is described in §6. We relate the stiffness of the suspension which is measured at the resonance of the pendulum to that at low frequency using the anelastic correction in §2:

$$\tau_c = n_{air}\left(1 - \frac{k_e}{k_g + k_e}\frac{2\Delta}{\pi}\ln\left\{\frac{T_m}{T_0}\right\}\right)I\left(\frac{2\pi}{T_0}\right)^2\Delta\theta_c. \tag{11.9}$$

We find the relative uncertainty in G for this method to be

$$\frac{\Delta G_c}{G} = \frac{\delta k(\omega_m)}{k} + \frac{\delta\Delta\theta_c}{\Delta\theta_c} - \left(\frac{\delta M}{M} + \frac{\delta m}{m} + \frac{4\delta r_a}{r} - 5\frac{\delta R_{ac}}{R} + 4\frac{\delta r_b}{r} - 5\frac{\delta R_b}{R} + \alpha_{cT}\right) + \frac{\delta\tau_c}{\tau}, \tag{11.10a}$$

where $\delta\tau_c$ is the random uncertainty owing to measurement noise and δR_{ac} is the uncertainty in the position of the source masses in the Cavendish experiment. A conservative estimate of a bias in $\delta k(\omega_m)$ equates it to the total correction for anelasticity that we apply to the final result for G in equation (11.9)

$$\delta k(\omega_m) = \delta k_r + \delta(I\omega_0^2) \tag{11.10b}$$

and

$$\delta k_r = \frac{k_e}{k_e + k_g}\frac{2\Delta}{\pi}\ln\left\{\frac{T_m}{T_0}\right\}. \tag{11.10c}$$

The moment of inertia comprises two terms

$$I = 4mr^2 + I_t, \tag{11.11}$$

where I_t is the moment of inertia due to the torsion balance without the test masses in place having an uncertainty δI_t. We can now rewrite equation (11.10a) as

$$\frac{\Delta G_c}{G} = \frac{\delta m}{m} + 2\frac{\delta r_a}{r} + 2\frac{\delta r_b}{r} + \frac{\delta I_t}{I} - 2\frac{\delta T_0}{T_0} + \frac{\delta k}{k_r} + \frac{\delta \Delta \theta_c}{\Delta \theta_c}$$
$$- \left(\frac{\delta M}{M} + \frac{\delta m}{m} + 4\frac{\delta r_a}{r} - 5\frac{\delta R_{ac}}{R} + 4\frac{\delta r_b}{r} - 5\frac{\delta R_{bc}}{R}\right) + \frac{\delta \tau_c}{\tau}, \tag{11.12a}$$

or finally

$$\frac{\Delta G_c}{G} = -\frac{\delta M}{M} - 2\frac{\delta r_a}{r} + 5\frac{\delta R_{ac}}{R} - \alpha_c - \delta \alpha_{cT} + \frac{\delta \Delta \theta_c}{\Delta \theta_c} - 2\frac{\delta T_0}{T_0} + \frac{\delta I_t}{I} + \frac{\delta k}{k_r} + \frac{\delta \tau_c}{\tau}, \tag{11.12b}$$

where T_0 is the period of free oscillation of the torsion balance.

(d) Combination of uncertainties

We can write the uncertainties for both measurements in matrix form

$$\begin{pmatrix} \delta G_s \\ \delta G_c \end{pmatrix} = \underline{\underline{A}}\, \underline{u}, \tag{11.13a}$$

where $\underline{u}$ is a vector of the values for the uncertainties in the parameters and $\underline{\underline{A}}$ is a matrix of the factors which multiply each component of the uncertainty. We use a shorthand notation where we write the fractional uncertainty $\delta p / p$ in parameter p as δp. We can write

$$A = \begin{pmatrix} -1 & -1 & -4 & 5 & 0 & -1 & -1 & 0 & 0 & -1 & 1 & 2 & 0 & 0 & 1 & 0 \\ 0 & -1 & -2 & 0 & 5 & 0 & 0 & -1 & -1 & 0 & 0 & 0 & 1 & 1 & 0 & 1 \end{pmatrix}, \tag{11.13b}$$

and the transpose of $\underline{u}$ is

$$u' = (\delta m \quad \delta M \quad \delta r_a \quad \delta R_{as} \quad \delta R_{ac} \quad \delta \alpha_s \quad \delta \alpha_{sT} \quad \delta \alpha_c \quad \delta \alpha_{cT} \quad \delta \Delta \theta_c \quad \delta \Delta C \quad \delta \Delta V \quad \delta I_t \quad \delta k_{0b} \quad \delta \tau_s \quad \delta \tau_c). \tag{11.13c}$$

The variances and covariances of the two values of G can then be written as

$$\begin{pmatrix} <\delta G_s^2> & <\delta G_s \delta G_c> \\ <\delta G_s \delta G_c> & <\delta G_c^2> \end{pmatrix} = \left\langle \begin{pmatrix} \delta G_s \\ \delta G_c \end{pmatrix} \begin{pmatrix} \delta G_s & \delta G_c \end{pmatrix} \right\rangle = \langle uAA^t u^t \rangle = \begin{pmatrix} \sigma_s^2 & \kappa \\ \kappa & \sigma_c^2 \end{pmatrix}, \tag{11.14a}$$

where the variances are

$$\sigma_s^2 = \sum_j A_{1j} A_{1j} \delta p_j^2 \tag{11.14b}$$

and

$$\sigma_c^2 = \sum_j A_{2j} A_{2j} \delta p_j^2, \tag{11.14c}$$

and the covariance is

$$\kappa = \sum_j A_{1j} A_{2j} \delta p_j^2. \tag{11.14d}$$

We can write a general combination of the values of G as

$$G_w = \lambda G_s + \mu G_c, \tag{11.15a}$$

with its uncertainty δG_w,

$$\delta G_w^2 = \lambda^2 \sigma_s^2 + 2\lambda \mu \kappa + \mu^2 \sigma_c^2. \tag{11.15b}$$

The uncertainty in the difference in the two values of G can be found by setting $\lambda = 1$ and $\mu = -1$. Using the values in table 1, we find $\delta G_{Diff} = 104$ ppm. As the measured difference between the values, as given in §12, is also 106 ppm this indicates that our statistical analysis is consistent with this difference and provides an, albeit crude, consistency check on our estimated uncertainties. Note that if the two methods were completely uncorrelated the uncertainty on their difference

Table 1. Values for the uncertainities on the parameters required to calculate G in equation (11.13c).

quantity	fractional uncertainty, ppm
test masses $\delta m/m$ (correlated)	1
source masses $\delta M/M$ (correlated)	1
test mass type A servo (correlated)	17
test mass type A Cavendish (correlated)	8
source mass type A for both servo and Cavendish (uncorrelated)	12
servo type B uncertainty for source and test masses $\delta\alpha_s$	4
Cavendish type B uncertainty for source and test masses $\delta\alpha_c$	−3
servo type A uncertainty for 0.1 K temperature change $\delta\alpha_{sT}$	−2
Cavendish type A uncertainty for 0.1 K temperature change $\delta\alpha_{cT}$	−7
angle measurement $\delta\Delta\phi/\Delta\phi$ (anti-correlated)	47
capacitance calibration $\delta\Delta C/\Delta C$	6
voltage calibration $2\,\delta V/V$	12
timing error $2\Delta T_0/T_0$	0.5
moment of inertia of torsion disc	13
anelasticity $\delta k/k_r$	6
uncertainty in mean servo torque $\delta\tau_s/\tau$	30
uncertainty in mean Cavendish torque $\delta\tau_c/\tau$	19
net uncertainty on servo value σ_s	61
net uncertainty on Cavendish value σ_c	54
covariance κ	−2080
correlation coefficient	−0.63

would be 81 ppm which is the quadrature sum of the uncertainties on each value. We can calculate an unbiased weighted mean by setting $\mu = 1 - \lambda$ [25] and by choosing a value of μ that minimizes equation (11.15b). Using the experimental values, we find $\delta G_{\mathrm{Comb}} = 25$ ppm with the weight for the servo and Cavendish results being 0.46 and 0.54, respectively. The values of the parameters are given in table 1.

12. A value for Newton's constant of gravitation

The peak-to-peak servo torque, τ_s, obtained as an unweighted mean of 10 data runs was $3.148869(94) \times 10^{-8}$ N m and using equations (9.2a) and (11.3) we can write

$$G_s = \frac{\tau_s}{\Gamma_s} = 6.67515(41) \times 10^{-11}\,\mathrm{m}^3\,\mathrm{kg}^{-1}\,\mathrm{s}^{-2}\ (61\,\mathrm{ppm}). \tag{12.1a}$$

The unweighted mean of the 10 data runs giving a value of the peak-to-peak deflection angle of $0.1529322(29)$ mrad using equations (9.2b), (8.2) and (11.8) we can write

$$G_c = \frac{\tau_c}{\Gamma_c} = 6.67586(36) \times 10^{-11}\,\mathrm{m}^3\,\mathrm{kg}^{-1}\,\mathrm{s}^{-2}\ (54\,\mathrm{ppm}). \tag{12.1b}$$

We have used the values for the uncertainties in the experimental measurements given in §11.

The weighted mean of the values is

$$G = 6.67554(16) \times 10^{-11} \, \text{m}^3 \, \text{kg}^{-1} \, \text{s}^{-2} \, (25 \, \text{ppm}). \tag{12.2}$$

The difference between the values amounts to 106 ppm. This is consistent with an uncertainty in this difference which is 104 ppm, as was calculated in the previous section.

This value of G differs from our published result [2] by 13 ppm (see erratum in [2]) due to

— an incorrectly applied correction for density homogeneity of -32 ppm to the Cavendish result; that correction had been included in Γ_c;
— a correction of -13 ppm for anelasticity with an uncertainty of 4 ppm, which we now believe should be a correction of -6 ppm with an uncertainty of 6 ppm; and
— an unnecessary correction of $+8$ ppm included in the calculation for G in both servo and Cavendish methods for an offset in the alignment of the source masses which should not exist because the alignment procedure eliminates such a misalignment. In addition, more accurately represented thermal effects in the dimensional metrology decreased the correlation coefficient from -0.58 to -0.63; this has reduced the uncertainty on the final value of G from 27 to 25 ppm.

13. Final remarks

In our 2013 paper, we remark that the value then given and that published in 2001 are statistically independent and that they are also statistically consistent. We also referred to the fact that each is based on the average of two largely independent methods, the servo and the Cavendish. At the start of this paper, in describing our method we said: *in an experiment in which there are two or more independent methods, one has first to look for errors in each until they all agree. When this is the case, the only errors that can remain are those in the much more limited set common to all.* We note again that in our experiments the servo method relies essentially on electrical and angle measurements while the Cavendish relies on timing and angle measurements, but that the same relative error in angle measurement produces equal but opposite effects in the two methods and is thus eliminated in the average of the two. Thus, it seems evident that if the servo and Cavendish results agree within their own uncertainties, this is strong evidence that unknown errors in electrical, angle and timing must be at or below the level of these uncertainties. The experiment will still, however, be subjected to unknown errors in other measured quantities that are common to both servo and Cavendish methods, notably in our case, dimensional metrology and source mass properties. But, the unknown errors in these parameters are the same in both the servo and Cavendish results. This would not be the case if the experiments were done separately.

We believe therefore that an experiment such as ours in which two methods were used gives added security and confidence in the results over and above that which can be obtained by a single method. We believe that this parallel process is more efficient, effective and less susceptible to bias than individual experimental teams working on one experimental configuration and comparing their result with those already published.

If the third, timing method could be successfully achieved, given a sufficiently stable temperature, this would give additional security, because it would depend essentially on timing. The principal common errors to all three methods would be (i) dimensional metrology and (ii) density uniformity of the source and test masses plus, of course, possible other errors of which we are unaware and which may have affected our present results by significant amounts.

and Mk II apparatus which were of the highest mechanical perfection without which none of this work would have been possible. We also thank participants in the Royal Society meeting for constructive and helpful discussions. We also wish to thank the referee for his very helpful suggestions.

References

1. Quinn TJ, Speake CC, Richman SJ, Davis RS, Picard A. 2001 A New determination of *G* using two methods. *Phys. Rev. Lett.* **87**, 111101. (doi:10.1103/PhysRevLett.87.111101)
2. Quinn TJ, Parks H, Speake CC, Davis RS. 2013 Improved determination of *G* using two methods. *Phys. Rev. Lett.* **111**, 101102. (doi:10.1103/PhysRevLett.111.101102) Erratum. 2014 *Phys. Rev. Lett.* **113**, 039901. (doi:10.1103/PhysRevLett.111.039901)
3. Cohen ER, Taylor BN. 1987 The 1986 adjustment of the fundamental constants. *Rev. Mod. Phys.* **59**, 1121–1148. (doi:10.1103/RevModPhys.59.1121)
4. Luther GG, Towler WR. 1982 Redetermination of the Newtonian gravitational constant *G*. *Phys. Rev. Lett.* **48**, 121–123. (doi:10.1103/PhysRevLett.48.121)
5. Michaelis W, Haars H, Augustin R. 1996 A new precise determination of Newton's gravitational constant. *Metrologia* **32**, 267–276. (doi:10.1088/0026-1394/32/4/4)
6. Boys CV. 1895 On the Newtonian constant of gravitation. *Phil. Trans. R. Soc. Lond. A* **186**, 1–72. (doi:10.1098/rsta.1895.0001)
7. Quinn TJ, Speake CC, Brown LM. 1992 Materials problems in the construction of long-period pendulums. *Philos. Mag.* **65**, 261–276. (doi:10.1080/01418619208201522)
8. Quinn TJ, Speake CC, Davis RS, Tew W. 1995 Stress-dependent damping in Cu–Be torsion and flexure suspensions at stresses up to 1.1 GPa. *Phys. Lett. A* **197**, 197–208. (doi:10.1016/0375-9601(94)00921-B) Erratum. 1995 *Phys. Lett. A* **198**, 474. (doi:10.1016/0375-9601(95)00095-K)
9. Quinn TJ, Davis RS, Speake CC, Brown LM. 1997 The restoring torque in wide Cu–Be torsion strips. *Phys. Lett. A* **228**, 36–42. (doi:10.1016/S0375-9601(97)00082-0)
10. Quinn TJ, Speake CC, Davis RS. 1997 Novel torsion balance for the measurement of the Newtonian constant of gravitation. *Metrologia* **34**, 245–249. (doi:10.1088/0026-1394/34/3/6)
11. Richman SJ, Quinn TJ, Speake CC, Davis RS. 1999 Preliminary determination of *G* using the BIPM torsion strip balance. *Meas. Sci. Technol.* **10**, 460–466. (doi:10.1088/0957-0233/10/6/308)
12. Speake CC, Quinn TJ, Davis RS, Richman SJ. 1999 Experiment and theory in anelasticity. *Meas. Sci. Technol.* **10**, 430–466. (doi:10.1088/0957-0233/10/6/303)
13. Speake CC, Gillies GT. 1987 Why is G the least precisely known physical constant? *Z. Naturforsch. A* **42**, 663–669.
14. Ledbetter HM. 1982 Temperature behaviour of Young's moduli of forty engineering alloys. *Cryogenics* **22**, 653–656. (doi:10.1016/0011-2275(82)90072-8)
15. Kuroda K. 1995 Does the time-of-swing method give a correct value of the Newtonian gravitational constant? *Phys. Rev. Lett.* **75**, 2796–2798. (doi:10.1103/PhysRevLett.75.2796)
16. Heyl PR, Chrzanowski P. 1942 A new determination of the constant of gravitation. *J. Res. Natl Bur. Stand.* **29**, 1–31. (doi:10.6028/jres.029.001)
17. Speake CC. 2005 Newton's constant and the 21st century laboratory. *Phil. Trans. R. Soc. A* **363**, 2265–2287. (doi:10.1098/rsta.2005.1643)
18. Smythe WH. 1989 *Static and dynamic electricity*, p. 76, 3rd edn. New York, NY: Hemisphere Publishing.
19. Leslie WHP. 1961 Choosing transformer ratio arm bridges. *Proc. IEE, Part B: Electron. Commun. Eng.* **108**, 539–545. (doi:10.1049/pi-b-2.1961.0093)
20. Speake CC, Davis RS, Quinn TJ, Richman SJ. 1999 Electrostatic damping and its effect on precision mechanical experiments. *Phys. Lett. A* **263**, 219–225. (doi:10.1016/S0375-9601(99)00597-6)
21. Michaelis W, Melcher J, Haars H. 2004 Supplementary investigations to PTB's evaluation of G. *Metrologia* **41**, L29–L32. (doi:10.1088/0026-1394/41/6/L01) Erratum. 2005 *Metrologia* **42**, 67. (doi:10.1088/0026-1394/41/1/C01)
22. D'Urso C, Adelberger EG. 1997 Translation of multipoles in a $1/r$ potential. *Phys. Rev. D* **55**, 7970–7972. (doi:10.1103/PhysRevD.55.7970)
23. Trenkel C, Speake CC. 1999 Interaction potential between extended bodies. *Phys. Rev. D* **60**, 107501. (doi:10.1103/PhysRevD.60.107501)
24. Chen YT, Cook AH. 1993 *Gravitational experiments in the laboratory*, p. 115. Cambridge, UK: Cambridge University Press.
25. Cox MG, Eiø C, Mana G, Penecchi F. 2006 Generalized weighted mean of correlated quantities. *Metrologia* **43**, S268–S275. (doi:10.1088/0026-1394/43/4/S14)